

---

This is the **accepted version** of the journal article:

Aller Pellitero, Miguel; Santiago, Sara; Ruiz, Jules; [et al.]. «Fully-printed and silicon free self-powered electrochromic biosensors : Towards naked eye quantification». Sensors and Actuators, B: Chemical, Vol. 306 (March 2020), art. 127535. DOI 10.1016/j.snb.2019.127535

---

This version is available at <https://ddd.uab.cat/record/274563>

under the terms of the  license

# **Fully-printed and silicon free self-powered electrochromic biosensors: towards naked eye quantification**

Miguel Aller Pellitero<sup>a</sup>, Sara Santiago-Malagón<sup>b</sup>, Jules Ruiz<sup>c</sup>, Yasmine Alonso<sup>b</sup>, Boris Lakard<sup>c</sup>, Jean-Yves Hihn<sup>c</sup>, Gonzalo Guirado<sup>b</sup>, F. Javier del Campo<sup>\*a</sup>

Electrochromic materials are becoming increasingly important in analytical devices and applications. Their opto-electronic properties make them particularly useful in the development of electronics-free, self-powered sensors. However, the mass manufacture of such devices is often limited by the need for transparent electrodes and liquid electrolyte systems. The self-powered biosensor presented here overcomes these limitations by means of a coplanar electrode construction and a gel electrolyte. This configuration enables an effective separation between the sample and the electrochromic component, which allows the naked eye readout of the analyte concentration even if coloured or dark samples, such as blood, are used. This lack of contact between sample and electrochromic material also prevents the action of possible interferences on the electrochromic display, which is an additional advantage. Moreover, because the device is entirely screen-printed, its mass production is also feasible. The fabricated device features a glucose biosensor connected to a Prussian-Blue electrode, displaying a dynamic range between 2.5 mM to 10 mM that makes it suitable for blood testing and diabetes screening.

**Keywords:** Glucose biosensor, Prussian Blue, Electrochromism, Gel electrolyte, Screen-printed electrodes.

<sup>a</sup>Instituto de Microelectrónica de Barcelona, IMB-CNM (CSIC), Campus de la Universidad Autónoma de Barcelona, Esfera UAB 08193-Bellaterra, Spain. \*E-mail: [javier.delcampo@csic.es](mailto:javier.delcampo@csic.es); Tel: +34 935947700

<sup>b</sup>Departament de Química, Facultat de Ciències, Universitat Autònoma de Barcelona, Esfera UAB 08193-Bellaterra, Spain.

<sup>c</sup>Institut UTINAM, UMR 6214 CNRS/Université de Franche-Comté, 16 route de Gray, 25030-Besançon, France.

## Introduction

Self-powered (bio)sensors are analytical devices able to produce their energy from their target analyte, yielding a power output that is proportional to the analyte concentration.[1-4] The main advantage of self-powered systems is that they do not require additional power sources. In the case of analytical systems, they take their power from the sample in direct proportion to analyte concentration. This simplifies device construction, reduces instrumentation needs to a minimum, and often facilitates portability, which is of particular relevance in point-of-care diagnosis.[5] However, barring exceptions, extracting the quantitative analytical information requires the use of electrochemical[6] or optical[7] readers.

Since the introduction of the self-powered sensors in 2001 by Katz and Willner,[1] most of the efforts done in this field have focused on improving the power output of these systems, making it sufficiently high and sustainable for long enough to power the signalling system and other possible components.[2] This has been achieved by optimizing the electrochemical cell design,[8] the biosensor performance,[9] or introducing new fabrication materials.[10]

An interesting alternative to the use of external detection systems is the construction of self-powered sensors using electrochromic materials.[11] Electrochromic materials are redox compounds presenting different optical properties as a function of their oxidation state.[12] The application of these materials in sensing applications has been the subject of recent reviews,[11, 13, 14] but their use in analytical devices, including self-powered, remains very limited.

Electrochromic materials were first introduced in self-powered analytical devices by Crooks and co-workers.[15] In that work, the authors presented a battery-powered paper-based glucose biosensor that enabled the detection of glucose above a concentration limit of 0.1 mM. The presence of glucose led to the reduction of a Prussian Blue (PB) spot to Prussian White (PW), enabling naked eye detection. Although this system only detects the presence of the analyte, its working principle could be transferred to many other electroanalytical assays that provide a “yes/no” answer, being also possible to achieve a semi-quantitative answer based on different concentration ranges.[16] Later studies relying on a similar working principle were reported but in these works an external optical reader was used to quantify the colour intensity changes of the electrochromic material, relating it to the analyte concentration. Jönsson-Niedziolka and co-workers presented a self-powered sensor for the quantification of ascorbic acid that used a biofuel cell to reversibly convert a PB display into its reduced form.[17] The amount of ascorbic acid was extracted from the display 100s after contact with the sample, using a camera and image analysis software. Similarly, Wang and co-workers reported a self-powered device for glucose

quantification based on a bipolar electrode.[18] One electrode end presented a glucose biosensor and the other a PB film. The reaction of the analyte in the biosensor bleaches the PB at a rate proportional to the analyte concentration, allowing to relate the amount of analyte with the extent of the discolouration. Recent works have reported on similar architectures but only with qualitative purposes.[19]

Conventional electrochromic displays use a “sandwich”, or parallel plate, configuration where anode and cathode directly face each other. This minimizes the ohmic drop between them and facilitates a faster and more homogeneous colour switch. A different, and much less exploited, approach for the construction of electrochromic displays is the “coplanar” or “interdigitated” configuration,[20] where anode and cathode rest on the same plane. Although using sufficiently conducting electrolyte results in nearly homogeneous colour changes, internal resistance can be used to generate the effect of colour gradients, providing a semi-quantitative, naked eye sensor readout.[11] Richardson,[21] Crooks,[22] and Gooding[23] pioneered the development of coplanar displays applied to the development of instrumentation-less readouts. This coplanar configuration has been only recently introduced by our group in the field of self-powered analytical devices.[24] This work presented a self-powered electrochromic device that used a PB display as a cathode to power the enzymatic reaction at the anode and also as a visual coulometer in the form of a metering bar, which enables the naked eye quantification of an analyte present in the solution flowing through a lateral flow membrane.

In addition, most electrochromic devices rely on the use of at least one transparent electrode. Tin-oxide materials[25] such as indium tin-oxide (ITO), antimony tin-oxide (ATO), or fluorine tin-oxide (FTO) as well as the polymeric mixture of poly(3,4-ethylenedioxythiophene) and polystyrene sulfonate[26] (PEDOT:PSS) are the most representative examples. In addition, thin layers of electrochromic materials are always deposited to ensure that, in the presence of an electrolyte with high ionic conductivity, a fast and reversible colour switch is obtained. While tin-oxide-based materials often perform better, their deposition in thin layers can be too costly. PEDOT:PSS, on the other hand, can be printed, which is more convenient, but its electrochromism may preclude observation of the desired colour change in some cases, so additional considerations are needed.

In this work, we have replaced the conventional transparent electrodes and the deposited thin layers of electrochromic material by a screen-printed layer based on semi-conducting antimony tin-oxide (ATO) particles coated with Prussian Blue.[27] A glucose biosensor was coupled to the electrochromic display in a coplanar arrangement so the system could work as a galvanic cell providing an easy to interpret colorimetric readout. Moreover, a formulated gel polymer

electrolyte based on an ionic liquid (IL) was printed on top of the PB display, replacing the conventional aqueous supporting electrolytes used in most electroanalytical experiments, and thus allowing to obtain a fully-printed solid-state analytical device.

## Experimental

### Chemicals and materials

The electroanalytical devices presented here were designed using VectorWorks 2018, Student Edition (Techlimits, ES). A 30 W Epilog Mini 24 CO<sub>2</sub> Laser engraver (Laser Project, ES) was used to cut the plastic substrates of polyethylene terephthalate (PET) with a nominal thickness of 500  $\mu\text{m}$  (Autostat WP20, MacDermid, UK). An Alpha-Step 200 profilometer from Tencor Instruments was used to measure the thickness of the different printed layers. Carbon (C2030519P4) and gold polymer (C2041206P2) screen-printing pastes were purchased from Gwent Electronic Materials Ltd. (UK), Electrodag silver (725A) and photocurable dielectric (PF-455B) pastes were obtained from Henkel (ES). Prussian Blue screen printing paste was prepared as previously described.[27] Ionic liquid 1-Ethyl-3-methylimidazolium trifluoromethanesulfonate (EMIM-Tf) was acquired from Solvionic (FR), potassium trifluoromethanesulfonate (KTf) and poly(vinylidene fluoride-*co*-hexafluoropropylene) (PVDF-HFP) were obtained from Sigma-Aldrich.

A  $\mu$ -Autolab III potentiostat from Metrohm controlled by GPES 4.1 software was used to carry out the electrochemical measurements. A SPELEC instrument by Metrohm-Dropsens (ES) was used to carry out spectroscopic measurements.

Glucose oxidase (GOx), EC 1.1.3.4, 236 U  $\text{mg}^{-1}$ , was purchased from Sekisui Diagnostics (UK). Poly(ethylene glycol) diglycidyl ether (PEGDGE), and glucose were obtained from Sigma-Aldrich. The redox polymer  $[\text{Os}(4,4'\text{-dimethyl-2,2'\text{-bipyridine}})_2(\text{poly-vinylimidazole})_{15}\text{Cl}]^+$  (Os-PVI<sub>15</sub>) used for the fabrication of the glucose biosensor was synthesized according to previous procedures.[28-30] A solution of 0.1 M potassium chloride (KCl) from Sigma-Aldrich and 0.05 M phosphate buffer (PBS) from Fluka was selected as the aqueous supporting electrolyte.

All reagents were used as received without any further purification.

### Electrode construction

Two types of screen-printed electrochemical cells were used in this work. The first cell consisted of a conventional 3-electrode design used to carry out electrochemical measurements (see S1). When needed, a Prussian Blue layer was printed on top of the carbon layer.[27] The second cell

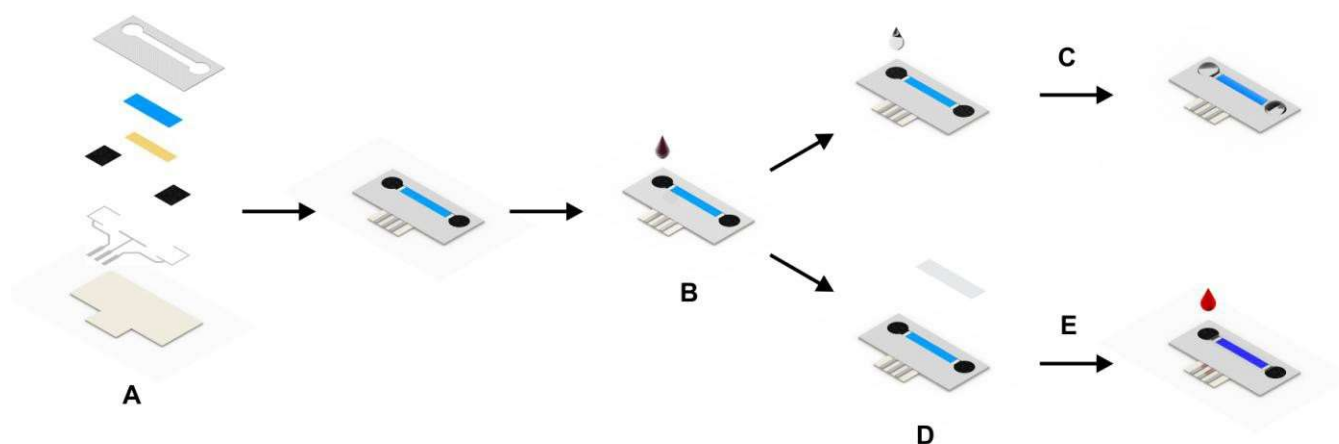


**Fig 1.** Schematic representation of the electrochromic analytical device fabrication. (A) Application of the different screen-printing pastes on the plastic substrate. (B) Modification of the carbon electrode with the components of the glucose biosensor. (C) Measurement using solutions of the aqueous supporting electrolyte covering both carbon electrodes and the PB display. (D) Printing of the gel polymer electrolyte covering the display and a small part of both carbon electrodes. (E) Measurement of a sample spread only on the surface of the carbon electrode modified with the glucose biosensor.

consisted of a printed Prussian Blue electrode of rectangular shape (2x15 mm) placed between two carbon electrodes, 5 mm in diameter each. Figure 1 outlines the fabrication steps of this electrochromic cell. First, silver conducting tracks were printed on the PET substrate. Next, the carbon paste was used to print the two working electrodes, one used as a transducer for the glucose biosensor, and the other used to regenerate the electrochromic display between measurements. A gold electrode was printed as a necessary step to improve the conductivity of the electrochromic layer printed on top,[31] and also to improve the colour contrast after the bleaching of the Prussian Blue. Last, a white colour dielectric layer was printed to define the electroactive areas of the cell. The surface of one of the carbon electrodes was modified to build the glucose biosensor, as described below. When required, a layer of gel polymer electrolyte was printed on top of the Prussian Blue electrode, slightly overlapping both carbon electrodes.

### Glucose biosensor fabrication

The surface of the working carbon electrode was modified to build the glucose biosensor. A protocol similar to that reported by Heller et al. was followed.[30] Briefly, 4  $\mu\text{L}$  of a 10  $\text{mg mL}^{-1}$  solution of the Os-PVI<sub>15</sub> prepared in a mixture of EtOH:H<sub>2</sub>O (1:1) were mixed with 0.8  $\mu\text{L}$  of a 10  $\text{mg mL}^{-1}$  solution of GOx prepared in the supporting electrolyte and 1.2  $\mu\text{L}$  of a 2.5  $\text{mg mL}^{-1}$  aqueous solution of PEGDE. 5  $\mu\text{L}$  were spread on the surface of the carbon electrode and allowed to dry at 4°C protected from ambient light. After 1 hour, the electrodes were ready for use. Blood glucose experiments were performed in compliance with CSIC's guidelines for experimentation

with humans and approved by CSIC's bioethics committee within the framework of the SEAMLESS project.

## **Gel polymer electrolyte**

The composition of the gel electrolyte was optimized to obtain a consistent, homogeneous, and transparent flexible layer. For this, an optimal weight ratio between the ionic liquid, the gelling polymer, and the amount of solvent was obtained. 0.14 g of the gelling agent, PVDF-HFP, was dissolved in 0.5 mL acetone under vigorous stirring and mild heating (40-50°C). After 15-30 minutes, a transparent solution is obtained, indicating the complete dissolution of the polymer. Then, 50 mg of KTf and 340  $\mu$ L of the IL were added to the mixture and stirred while heating for another 15 minutes. After this, the gel polymer was ready for printing. The thicknesses of the printed layers of gel polymer were measured with a profilometer, leading to values ranging between 10 and 20  $\mu$ m.

## **Results and Discussion**

### **Display characterization**

The shift from an electrodeposited PB layer,[24] which thickness is in the range of a few hundred nanometers, to a printed display where the thickness is closer to ten microns, results in changes to its electrochemical and optical properties. Figure 2 shows cyclic voltammograms recorded for two different Prussian Blue electrodes, one with a thin electrodeposited layer on a transparent ITO electrode on a glass substrate,[24] and the other with a thick printed layer on top of a screen-printed gold electrode as shown in Figure 1, using in both experiments the same aqueous supporting electrolyte. As expected, the amount of electrochromic material per unit area is much higher in the case of the printed display (8.9  $\text{mC cm}^{-2}$  vs 2.7  $\text{mC cm}^{-2}$ , respectively). This increase in the amount of PB results in a slower apparent response, despite the ~~semi~~-relatively-conducting nature of the ATO microparticles underneath the PB coating. Thus, peak-to-peak separation increases from 30 mV in the case of the electrodeposited layer to roughly 60 mV for the printed layer. The higher amount of electrochromic material as well as the more sluggish electron transfer alter the behaviour of the display. For this, the nature and properties of the selected electrolyte must be adjusted in order to obtain a fast and clear colour switch.[32] To study the behaviour of the PB display under different electrolyte conditions, a constant electric current of 40  $\mu$ A was applied from the working electrode so the PB was progressively converted into PW. Two aqueous electrolytes with different conductivities were used. One, a 0.1 M KCl aqueous solution with high

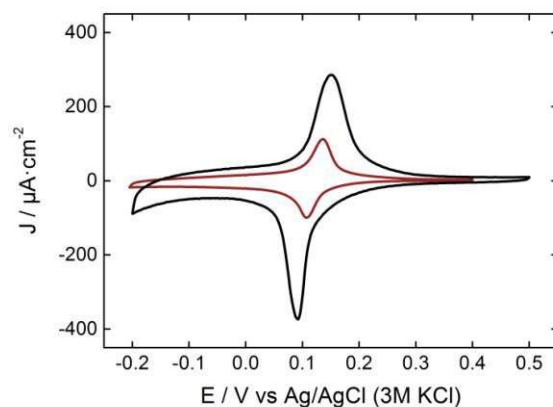


**Fig. 2** Cyclic voltammograms of electrodeposited (red line) and printed (black line) PB electrodes using in both cases an aqueous supporting electrolyte. Scan rate of  $5 \text{ mV s}^{-1}$ .

conductivity similar to those used in common electroanalytical experiments,  $\sigma_1 = 1.6 \text{ S m}^{-1}$ , and the other, a  $0.01 \text{ M KCl}$  solution with much lower conductivity,  $\sigma_2 = 0.16 \text{ S m}^{-1}$ . Also, the electrolyte resistance was manually controlled by depositing different volumes of solution, thus adjusting the thickness of the electrolyte on the electrode surface so two different electrolyte volumes heights of electrolyte could be tested, namely  $H_1 \approx 2 \text{ mm}$  and  $H_2 \approx 0.1 \text{ mm}$ , where  $H$  represents the height of the electrolyte volume.  $H_1 \approx 2 \text{ mm}$  aimed at simulating providing the conditions of a system in which the current lines are distributed through the thick layer of the ionic conductor, while  $H_2 \approx 0.1 \text{ mm}$  aimed at simulation modeling a printed layer of electrolyte in which the current lines are restricted to a smaller volume. As seen in Figure 3, when an electrolyte with high conductivity is selected and a high volume is deposited on the surface of the electrodes, the electrochromic display switches colour homogeneously across its entire surface, and a full conversion from PB to PW is observed. If either the electrolyte conductivity or its thickness decreases, the internal resistance of the solution increases, and the electric current, which follows the path of least resistance, progressively depletes the electrochromic material at the display, generating a colour gradient. Last, when both electrolyte conductivity and thickness decrease, the internal resistance increases even more, resulting in two effects. First, the colour front is better defined due to the abrupt  $iR$  drop at the switching region, and second, the conversion rate of the PB is considerably slower. It is important to note that, under these stringent conditions, the electrochromic display can be irreversibly damaged by the degradation of either the ATO core of the particles or the electrochromic coating.



The galvanostatic experiments of-shown in Figure 3 show demonstrate that an electrolyte with intermediate properties between the cases 'iii' and 'iv', where the colour conversion is better defined, may lead to an optimum display performance, i.e., fast and clear colour conversions. When considering possible printable electrolytes that fulfill this, two important points must be taken into account. First, it is necessary to control the deposition of the electrolyte on the device since, as shown above, the thickness of the layer plays a critical effect on its performance, leading to considerable variations in rate and definition of colour conversions. Moreover, it is desirable that the device is able to measure in any kind of sample, regardless of its colour, turbulence, or the presence of substances that may interfere with the electrochromic material, i.e., sample and display should be physically separated. In this sense, ionic liquid-based gel polymer electrolytes represent an interesting alternative to conventional aqueous electrolytes. IL-based gel electrolytes display relatively high ionic conductivities,[33] they can be screen-printed as any other paste, which allows to control the thickness of the material deposited and additionally, and, given their organic nature, they provide a very suitable separation barrier between sample and display, which allows ion exchange between the two phases without mixing.

### Gel electrolyte characterization

Solid-state electrolytes display certain advantages over conventional liquid electrolytes that make them a suitable option for printed electrochromic devices. These features include the outstanding mechanical stability, simplicity of fabrication and assembly of the devices, or the protection against possible leakages of toxic chemical compounds present in them.[33] Among the different types of solid-state electrolytes, gel polymer electrolytes stand out because of their relatively high conductivities.[34, 35] Particularly, ionic liquid-based gel polymer electrolytes display high ionic conductivities, besides other features such as non-volatility and wide potential windows.[36, 37] A suitable gel polymer electrolyte for electrochromic displays must show high ionic conductivity and high mechanical stability, in addition to a high degree of transmissivity. Moreover, the

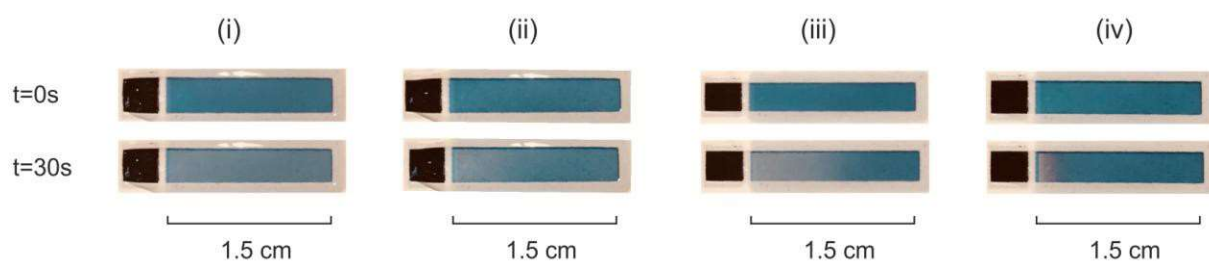


**Fig 3.** Captures of the display at two different times under a constant applied current of 40  $\mu\text{A}$  for different aqueous electrolyte conductivities ( $\sigma$ ) and thicknesses (H): (i)  $\sigma_1=1.6 \text{ S m}^{-1}$ ,  $H_1 \approx 2 \text{ mm}$ ; (ii)  $\sigma_2=0.16 \text{ S m}^{-1}$ ,  $H_2 \approx 2 \text{ mm}$ ; (iii)  $\sigma_1=1.6 \text{ S m}^{-1}$ ,  $H_2 \approx 0.21 \text{ mm}$ ; (iv)  $\sigma_2=0.16 \text{ S m}^{-1}$ ,  $H_2 \approx 0.1 \text{ mm}$ .

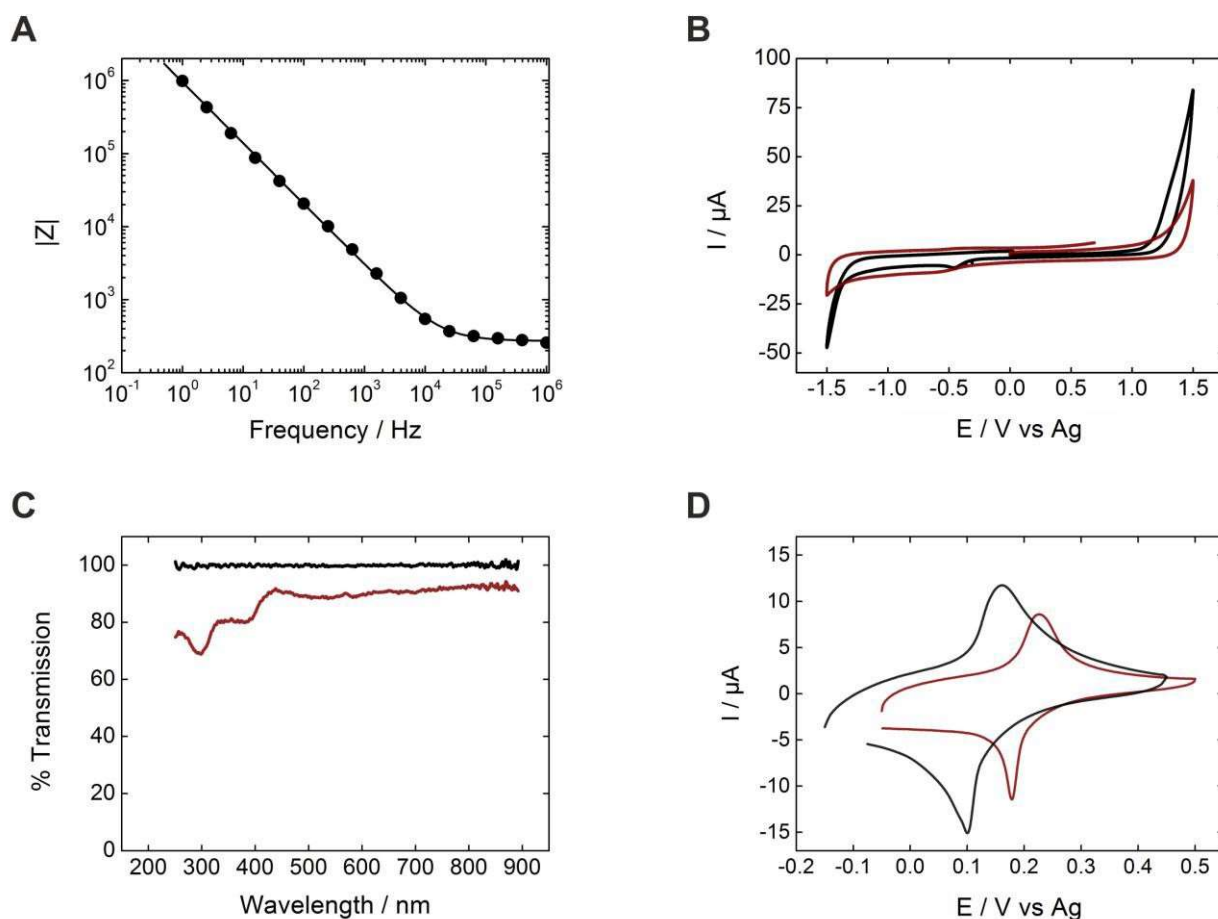


**Fig 4.** (A) Bode plot for the gel polymer electrolyte. Experimental data (circles), and fitted data obtained from the equivalent circuit (line). (B) Cyclic voltammograms obtained in a C-SPE (see Fig. S1) with a gel polymer electrolyte (red line) and an aqueous 0.1 M KCl solution (black line). Scan rate of 10 mV s<sup>-1</sup>. (C) UV-vis reflectance spectrum of a printed layer of gel polymer electrolyte (red line) compared to the background with no sample (black line). (D) Cyclic voltammograms obtained in a PB-SPE (see Fig. S1) with a gel polymer electrolyte (red line) and an aqueous 0.1 M KCl solution (black line). Scan rate of 5 mV s<sup>-1</sup>.

selected electrolyte must possess rheologic properties adequate for printing.

The formulated gel polymer consisted of a mixture of three components: an ionic liquid, EMIM-Tf, that served as ionic charge carrier, potassium trifluoromethanesulfonate, as the source of potassium required by the Prussian Blue to keep its reversibility,[38] and a fluoropolymer, PVDF-HFP, that was used as a gelling agent to provide consistency to the electrolyte in the form of a flexible and transparent gel where the other components of the mixture were embedded.

The physicochemical properties of the gel polymer electrolyte were studied. Its ionic conductivity was estimated by electrical impedance spectroscopy, using interdigitated electrodes (IDEs) of a 10x10  $\mu m$  geometry.[39] For this, 10  $\mu L$  of the polymer electrolyte was cast on the surface of the IDEs and let to dry, and the AC impedance response was registered. To analyse the impedance response, an equivalent circuit consisting of a constant phase element (CPE) representing the electrode/electrolyte interface in series with a resistance ( $R_s$ ) representing electrolyte resistance between electrodes was considered. As seen in Figure 4a, experimental and simulated data show an excellent fit, validating the implemented equivalent circuit. The

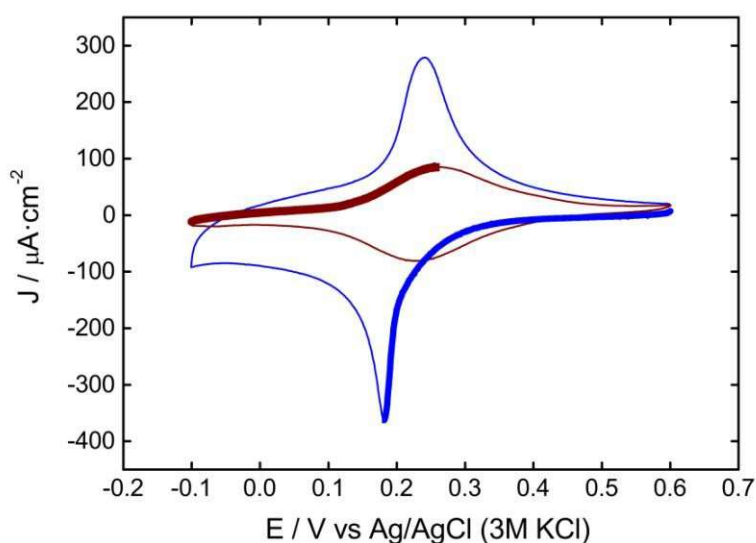


**Fig 5.** Cyclic voltammograms of the electroactive species at the anode, Os-PVI<sub>15</sub> (red line), and at the cathode, PB (blue line). The regions in bold highlight the electrode processes taking place during device operation. Scan rate of 5 mV s<sup>-1</sup>.

magnitude of the electrolyte resistance was obtained at high frequencies from the Bode plot, where the main contribution to the registered impedance values is due to the electrolyte resistance.[40] The obtained values for the resistance were interpolated with those obtained with the same IDEs in each case in aqueous KCl solutions of different conductivities, and an equivalent electrolyte conductivity of  $0.4 \pm 0.1 \text{ S m}^{-1}$  was estimated, in line with previously reported gel electrolytes of similar compositions.[41]

It is important that the selected electrolyte shows a wide electrochemical window, as is the case for the present ionic liquid gel polymer electrolyte. Figure 4b shows cyclic voltammograms for the gel polymer electrolyte and for the aqueous supporting electrolyte using screen-printed carbon electrodes (C-SPE). Although a wider potential window was expected due to the use of an ionic liquid, the gel polymer electrolyte displays a potential window similar to that of the aqueous electrolyte. We believe this is due to the water present in the ionic liquid or the acetone used to prepare the ionogel. However, no redox activity is observed in the range from 0 to 0.5 V vs  $\text{Ag}/\text{Ag}^+$ , where the PB/PW couple reacts, so this electrolyte system was accepted for this application.

As explained above, a very important feature that any suitable electrolyte must fulfil for its use in electrochromic devices/sensors is to display a high degree of optical transmissivity. The use of an ionic liquid in the formulation of the gel polymer electrolyte not only provides the required ionic conductivity, but it also confers the resulting gel the optical transparency sought in this case. Figure 4c shows the wavelength spectrum obtained on a PET substrate in a UV-vis reflectance

mode for a printed layer of the gel polymer electrolyte of roughly 15  $\mu\text{m}$ . As observed, no significant amount of light is absorbed in the visible region, obtaining transmission values, on average, higher than 90%.

Last, the electrochemical performance of the Prussian Blue paste was evaluated under the use of the gel electrolyte. For this, cyclic voltammograms were recorded with the PB screen-printed electrodes (PB-SPE) of Figure S1 using a 0.1M KCl aqueous solution or a pellet of gel electrolyte with a thickness of roughly 3 mm. As seen in Figure 4d, a shift in the position of the voltammograms appears due to the different anions present in each electrolyte, which affects the pseudo-reference  $\text{Ag}/\text{Ag}^+$  electrode potential. Also, peak currents decrease when using the polymer electrolyte since the diffusion coefficient of potassium is affected by the composition of the solution, as predicted by the Randles-Sevcik equation.[40] Regardless of this, the electrochemical performance of the electrochromic material with a gel polymer electrolyte is still remarkable.

As explained, an electrolyte with a conductivity lower than that of common aqueous solutions with a thin layer spread above the display should give rise to a better-defined colour transition, but maintaining a high conversion rate. Indeed, this was observed throughout the experiments run in the next section, when the system works as an enzymatic fuel cell.

### Self-powered device

The feasibility of any electrochemical system to work as a galvanic cell can be first assessed by looking at the cyclic voltammograms of the electrode processes involved. Figure 5 shows cyclic voltammograms recorded for the osmium redox polymer at the anode and for the Prussian Blue at the cathode. The onset potential of the PB reduction at the cathode is observed at 0.3 V vs  $\text{Ag}/\text{Ag}^+$ , while the oxidation of the osmium redox polymer is observed at 0.1 V vs  $\text{Ag}/\text{Ag}^+$ , which, in the absence of glucose, leads to cell voltages of roughly 0.2 V. Although the presence of glucose converts completely the redox mediator into its reduced state, and thus increases the cell voltage up to 0.5 V (Fig. 6A), these values are. ~~This cell voltage is~~ rather low compared to state-of-the-art enzymatic fuel cells,[42] and ~~it~~ this might have been a limiting factor in a conventional system, i.e, if powering a silicon-based electronic circuit had been required. However, in this case it just means a slower system response, or a somewhat limited device performance, particularly in systems with relatively high internal resistance.[32] The substitution of either the redox mediator or the electrochrome, or even both, by others with lower and higher formal potentials respectively, will lead to higher cell voltages, and thus to a better system both in terms of response time and dynamic range.

The behaviour of the self-powered system was studied under the use of either the aqueous or the gel polymer electrolyte, using glucose solutions of different concentration. The Prussian Blue cathode was connected to the sensing anode, and the electric current was registered scanning the potential from the open circuit value to the short circuit. Figure 6 shows the polarization and power curves corresponding to the systems with an aqueous electrolyte ('A' and 'B') and with a gel polymer electrolyte ('C' and 'D'). A progressive increase in the current and power output is observed as the amount of analyte is increased, reaching maximum values at 10 – 15 mM, in agreement with the amperometric calibration plot in Figure S2. The effect of the higher internal resistance in the fully printed device is observed when the maximum current output of both systems is compared. While the cell with an aqueous electrolyte reaches a maximum current density of roughly  $60 \mu\text{A cm}^{-2}$  at 20 mM glucose, the system with the gel polymer electrolyte is only capable of achieving  $35 \mu\text{A cm}^{-2}$ . Although this is approximately half of that generated by the aqueous electrolyte, the system still works relatively well.

Last, anode and cathode were short-circuited, and the progressive conversion of Prussian Blue in the display into its reduced form by action of the enzymatic activity was registered, measuring the distance converted after a fixed amount of time. The transition from an electrodeposited display of previous prototypes[24] to a printed one, as well as the proximity in the formal potential of the electroactive species involved in the cell makes it necessary to extend the measuring up to 90 seconds. Moreover, the shift from an aqueous to a gel polymer electrolyte with higher internal resistance, further increases the measuring time up to 5 minutes, since the conversion rate of the display is markedly slower. It was observed that the concentration of PVDF-HFP and ionic liquid in the paste, which determines the thickness of the printed layer of electrolyte, were critical parameters in the performance of the device. For this, the amount of solvent, acetone, was reduced to a minimum, compared to other gel polymer electrolytes with similar chemical compositions,[41] which allowed us to print thicker layers of material, leading to a substantial decrease in the measuring time from 20 to 5 minutes. This indicates that an improved formulation of the gel electrolyte, or optimized printing parameters such as screen mesh density[43] could lead to an improved performance of the device, reducing the measuring time even further. Also, as mentioned above, the substitution of the electroactive species at both electrodes by others that generate higher cell voltages would lead to similar results.

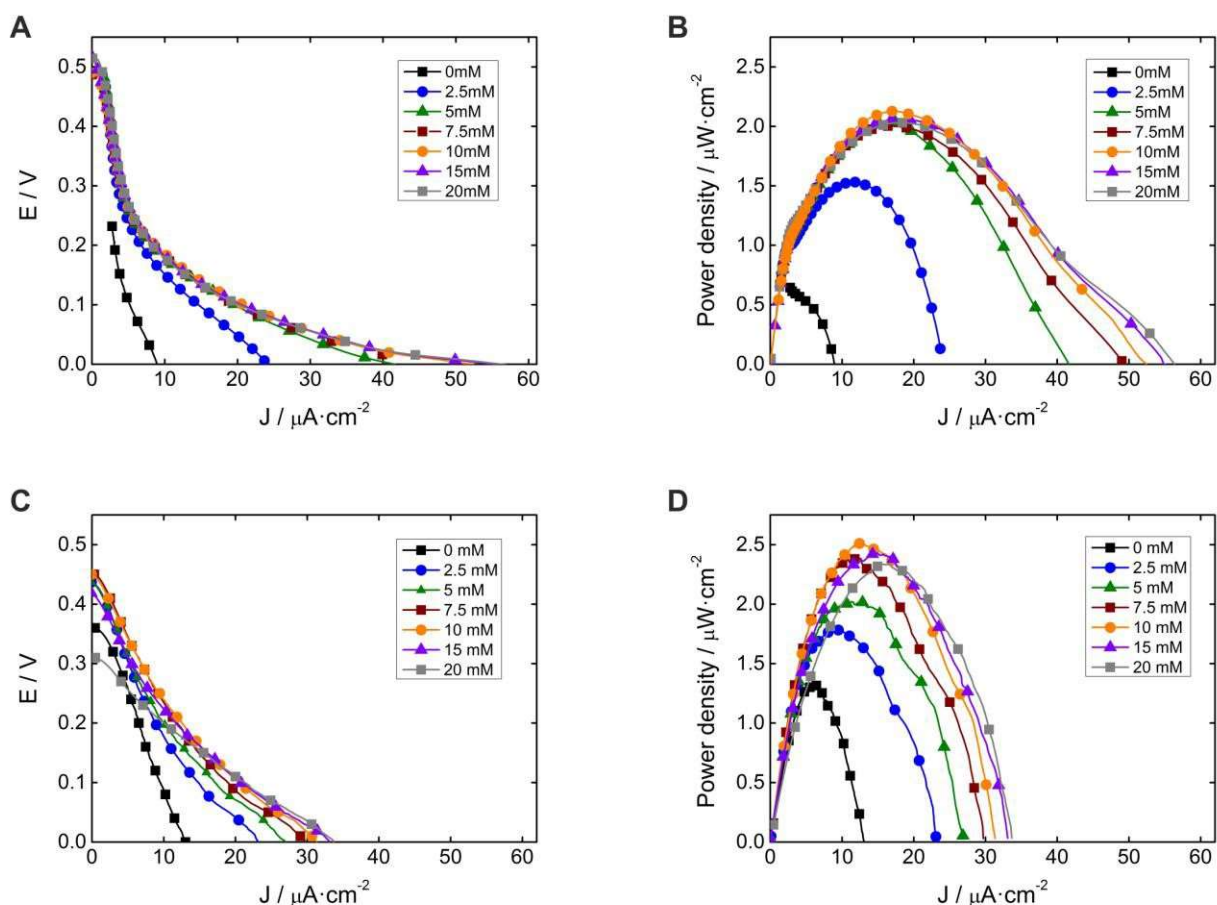


**Fig 6.** Polarization and corresponding power curves obtained for the self-powered device for different glucose concentrations using an aqueous (A and B) or a gel polymer (C and D) electrolyte. Scan rate of  $1 \text{ mV s}^{-1}$ .

Figure 7 shows images taken 90 seconds (aqueous electrolyte), ~~and~~ or 5 minutes (gel polymer electrolyte) after the connection of the electrodes ~~for the aqueous and gel polymer electrolyte, respectively~~. The points in the calibration curves represent the position of the colour front estimated from the images captured. A ~~clear~~ correlation between the distance converted and the concentration of glucose is observed in both systems. As expected, the colour transition observed in these devices is noticeably blurrier than in the case of an electrodeposited PB electrode, as a thicker electrochromic coating leads to lesser control over current line distribution. This effect is partially mitigated when the internal resistance of the cell is increased, for example, using a thinner layer of electrolyte of lower conductivity (Fig. 7A and B). Despite this improvement in colour definition, an appropriate selection of materials and reagents, i.e. redox mediator, electrochrome, or electrolyte, as well as different geometric architectures should be evaluated to ease the naked-eye readout of the display.

As mentioned above, one important advantage of using a printed gel polymer electrolyte instead of the conventional aqueous supporting electrolyte is the possibility of separating the sample from the electrochromic display, which allows to measure coloured samples that

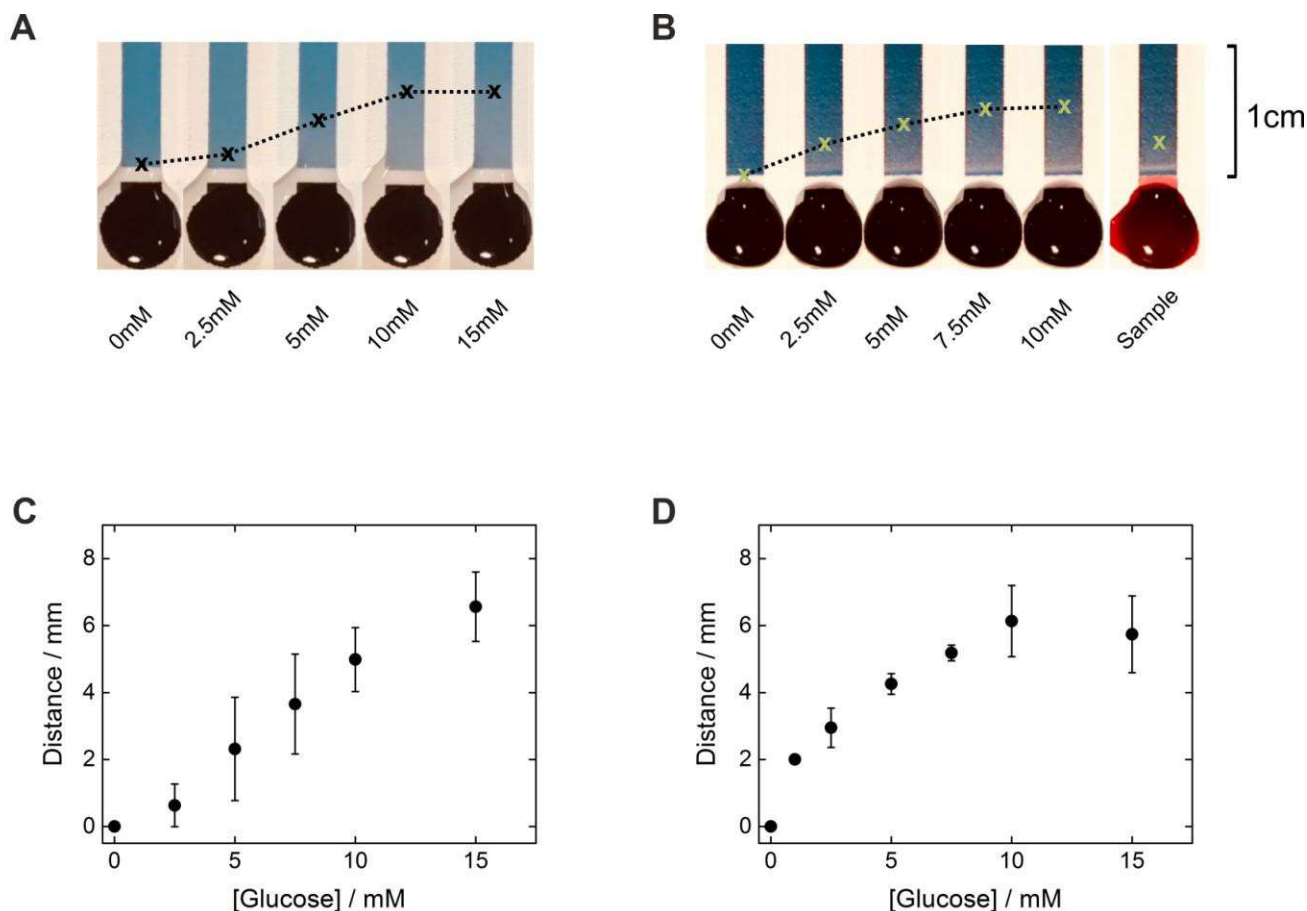


**Fig 7.** Captures of the evolution of the PB display after 90 seconds (A), and after 5 minutes (B) of connection of the system for different glucose concentrations prepared in supporting electrolyte, and for a human blood sample. (C) Calibration plot of the distance converted obtained from 'A'. (D) Calibration plot of the distance converted from 'B'. Error bars represent the standard deviation for  $n=3$  devices.

otherwise would mask the conversion of Prussian Blue into Prussian White, as well as to prevent the action of electroactive interferences on the display. To test this feature, human blood samples were collected from a volunteer's thumb using safety lancets. 15  $\mu\text{L}$  were extracted and placed on top of the biosensing anode, and the system was connected. As shown in Figure 7, the electrochromic display reaches a distance conversion slightly higher than that of the 2.5 mM glucose standard, in agreement with the measured concentration of 2.8 mM obtained using a commercial glucose meter (CardioCheck, Novalab, ES).

It is interesting to note that, while the device with the gel polymer electrolyte requires roughly 5 minutes to obtain a similar degree of colour conversion compared to the device with the aqueous electrolyte, the possibility of having a better control on the thickness of the electrolyte, and thus on the internal resistance of the cell, leads to a significant improvement in the repeatability of the measurements with different devices, as inferred by the size of the error bars, which are shorter.

Moreover, the colour conversion of the electrochromic display under the use of the two electrolytes was compared when the system was connected using a 15 mM glucose solution.



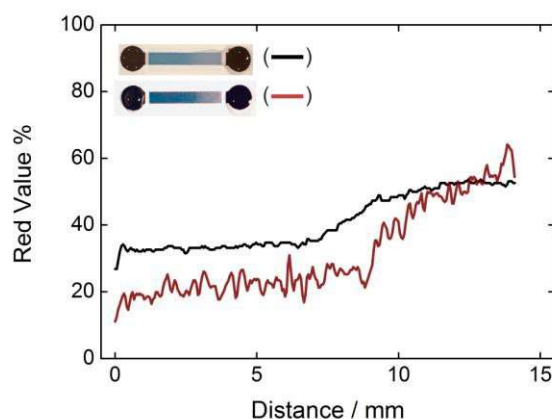


**Fig 8.** Colour profiles of the PB display obtained with ImageJ for the self-powered experiment with a 15 mM glucose solution under the use of the two electrolytes: aqueous (black line), and gel polymer (red line). Images were captured after 90 seconds and 5 minutes for the aqueous and gel-polymer electrolyte, respectively.

Figure 8 shows the percentage of the red channel values extracted from the RGB plots of both cases using image analysis software ImageJ (see Fig. S3 for a description of the methodology used to extract the RGB profiles).[44] As observed, the profile of the colour switch in the case of the gel electrolyte displays a steeper slope than that of the aqueous electrolyte. The thin printed layer of gel polymer and its lower ionic conductivity lead to a higher internal resistance, which translates into a better-defined colour conversion.

## Conclusions

In this work we have shown the fabrication of a self-powered electrochromic analytical device for the quantification of glucose entirely by screen-printing.

An electrochromic Prussian Blue paste was used to print the display/cathode, substituting conventional thin-layer electrodeposited PB electrodes, and removing the need for a transparent electrode.

An ionic liquid-based gel polymer was used to print a solid-state electrolyte substituting conventional aqueous electrolytes. The behaviour of the printed device under the use of the gel polymer electrolyte was evaluated and compared to that with a conventional supporting electrolyte. The use of a printable gel electrolyte allows the physical separation of the sample from the electrochromic display, avoiding the action of possible interfering substances. Moreover, since the sample does not contact the Prussian Blue display, it is possible to measure coloured samples that would otherwise mask the colour switch. The thin printed layer of electrolyte results in a higher internal resistance than in the case of an aqueous electrolyte, which increases the



measuring time. However, a better-defined colour conversion is achieved, facilitating the readout of the display.

The fabrication of a solid-state electrochromic sensing device entirely by screen-printing can lead to extremely cost effective devices including skin patches, contact lenses, and other non-invasive and easy to use wearables. [45-47]

## Conflicts of interest

There are no conflicts of interest to declare.

## Acknowledgements

MAP and SSM are supported by FEDER funds managed by the Catalan Secretary of Universities and Research through project PROD-0000114 (Enterprise and Knowledge, Industry Department, Generalitat de Catalunya). GG and SSM thank also financial support from the MINECO/FEDER CTQ2015-65439-R project. JdC gratefully acknowledges financial support through a 2016 Leonardo grant from the BBVA Foundation. The authors are grateful to Milliken for providing the electroconductive powders (ECPs) used to manufacture the electrochromic PB pigment. Zelec materials by Milliken provide cost-effective, static-dissipative performance for coatings and polymers. They are non-volatile, non-corrosive, and resistant to heat, chemicals and humidity. Zelec enhances quality and durability by imparting resistivity throughout the lifetime of coatings, paints, security inks and products.

## References

- [1] E. Katz, A.F. Bückmann, I. Willner, Self-Powered Enzyme-Based Biosensors, *J. Am. Chem. Soc.*, 123 (2001) 10752-3.
- [2] M. Grattieri, S.D. Minteer, Self-Powered Biosensors, *ACS Sensors*, 3 (2018) 44-53.
- [3] L. Fu, J. Liu, Z. Hu, M. Zhou, Recent Advances in the Construction of Biofuel Cells Based Self-powered Electrochemical Biosensors: A Review, *Electroanalysis*, 30 (2018) 2535-50.
- [4] S. Zhang, F. Cicoira, Flexible self-powered biosensors *Nature*, 561 (2018) 466-7.
- [5] C. Gonzalez-Solino, M.D. Lorenzo, Enzymatic Fuel Cells: Towards Self-Powered Implantable and Wearable Diagnostics, *Biosensors*, 8 (2018) 11.
- [6] D. Grieshaber, R. MacKenzie, J. Vörös, E. Reimhult, Electrochemical biosensors - Sensor principles and architectures, *Sensors*, 8 (2008) 1400-58.
- [7] S.M. Borisov, O.S. Wolfbeis, Optical biosensors, *Chem. Rev.*, 108 (2008) 423-61.
- [8] L. Doherty, X. Zhao, Y. Zhao, W. Wang, The effects of electrode spacing and flow direction on the performance of microbial fuel cell-constructed wetland, *Ecol. Eng.*, 79 (2015) 8-14.
- [9] D.P. Hickey, R.C. Reid, R.D. Milton, S.D. Minteer, A self-powered amperometric lactate biosensor based on lactate oxidase immobilized in dimethylferrocene-modified LPEI, *Biosens. Bioelectron.*, 77 (2016) 26-31.
- [10] R.L. Arechederra, S.D. Minteer, Self-powered sensors, *Anal. Bioanal. Chem.*, 400 (2011) 1605-11.
- [11] M.A. Pellitero, F.J. del Campo, Electrochromic sensors: Innovative devices enabled by spectroelectrochemical methods, *Curr. Opin. Electrochem.*, 15 (2019) 66-72.

[12] P.M.S. Monk, R.J. Mortimer, D.R. Rosseinsky, *Electrochromism: Fundamentals and Applications* 1995.

[13] A.A. Karyakin, Advances of Prussian blue and its analogues in (bio)sensors, *Curr. Opin. Electrochem.*, 5 (2017) 92-8.

[14] R. Celiesiute, A. Ramanaviciene, M. Gicevicius, A. Ramanavicius, *Electrochromic Sensors Based on Conducting Polymers, Metal Oxides, and Coordination Complexes*, *Crit. Rev. Anal. Chem.*, 49 (2019) 195-208.

[15] H. Liu, R.M. Crooks, Paper-Based Electrochemical Sensing Platform with Integral Battery and Electrochromic Read-Out, *Anal. Chem.*, 84 (2012) 2528-32.

[16] F. Zhang, T. Cai, L. Ma, L. Zhan, H. Liu, A paper-based electrochromic array for visualized electrochemical sensing, *Sensors* (Switzerland), 17 (2017).

[17] A. Zloczewska, A. Celebanska, K. Szot, D. Tomaszewska, M. Opallo, M. Jönsson-Niedziolka, Self-powered biosensor for ascorbic acid with a Prussian blue electrochromic display, *Biosens. Bioelectron.*, 54 (2014) 455-61.

[18] X. Zhang, L. Zhang, Q. Zhai, W. Gu, J. Li, E. Wang, Self-Powered Bipolar Electrochromic Electrode Arrays for Direct Displaying Applications, *Anal. Chem.*, 88 (2016) 2543-7.

[19] X. Yu, J. Liang, T. Yang, M. Gong, D. Xi, H. Liu, A resettable and reprogrammable keypad lock based on electrochromic Prussian blue films and biocatalysis of immobilized glucose oxidase in a bipolar electrode system, *Biosens. Bioelectron.*, 99 (2018) 163-9.

[20] J.P. Coleman, A.T. Lynch, P. Madhukar, J.H. Wagenknecht, Printed, flexible electrochromic displays using interdigitated electrodes, *Sol. Energy Mater. Sol. Cells*, 56 (1999) 395-418.

[21] G. Chen, T.J. Richardson, Overcharge protection for high voltage lithium cells using two electroactive polymers, *Electrochem. Solid-State. Lett.*, 9 (2006) A24-A6.

[22] K.-F. Chow, B.-Y. Chang, B.A. Zaccaro, F. Mavr , R.M. Crooks, A Sensing Platform Based on Electrodissolution of a Ag Bipolar Electrode, *J. Am. Chem. Soc.*, 132 (2010) 9228-9.

[23] D.D. Liana, B. Raguse, J.J. Gooding, E. Chow, Toward Paper-Based Sensors: Turning Electrical Signals into an Optical Readout System, *ACS Appl. Mater. Interfaces*, 7 (2015) 19201-9.

[24] M.A. Pellitero, A. Guimera, M. Kitsara, R. Villa, C. Rubio, B. Lakard, et al., Quantitative self-powered electrochromic biosensors, *Chem. Sci.*, 8 (2017) 1995-2002.

[25] A. Kumar, C. Zhou, The Race To Replace Tin-Doped Indium Oxide: Which Material Will Win?, *ACS Nano*, 4 (2010) 11-4.

[26] R. Singh, J. Tharion, S. Murugan, A. Kumar, ITO-Free Solution-Processed Flexible Electrochromic Devices Based on PEDOT:PSS as Transparent Conducting Electrode, *ACS Appl. Mater. Interfaces*, 9 (2017) 19427-35.

[27] M.A. Pellitero, J. Freneau, R. Villa, G. Guirado, B. Lakard, J.-Y. Hihn, et al., Electrochromic biosensors based on screen-printed Prussian Blue electrodes, *Sens. Actuators B Chem.*, 290 (2019) 591-7.

[28] D.A. Buckingham, F.P. Dwyer, H.A. Goodwin, A.M. Sargeson, Mono and Bis-(2,2'-bipyridine) and (1,10-phenanthroline) chelates of ruthenium and osmium, *Aus. J. Chem.*, 17 (1964) 325-36.

[29] R.J. Forster, J.G. Vos, Synthesis, Characterization, and Properties of a Series of Osmium and Ruthenium-Containing Metallopolymers, *Macromolecules*, 23 (1990) 4372-7.

[30] T.J. Ohara, R. Rajagopalan, A. Heller, Wired enzyme electrodes for amperometric determination of glucose or lactate in the presence of interfering substances, *Anal. Chem.*, 66 (1994) 2451-7.

[31] M.A. Pellitero,  . Colina, R. Villa, F.J. del Campo, Antimony tin oxide (ATO) screen-printed electrodes and their application to spectroelectrochemistry, *Electrochem. Comm.*, 93 (2018) 123-7.

[32] M.A. Pellitero, A. Guimer , R. Villa, F.J. del Campo, iR Drop Effects in Self-Powered and Electrochromic Biosensors, *J. Phys. Chem. C*, 122 (2018) 2596-607.

[33] D.P. Dubal, N.R. Chodankar, D.H. Kim, P. Gomez-Romero, Towards flexible solid-state supercapacitors for smart and wearable electronics, *Chem. Soc. Rev.*, 47 (2018) 2065-129.

[34] J.Y. Song, Y.Y. Wang, C.C. Wan, Review of gel-type polymer electrolytes for lithium-ion batteries, *J. Power Sources*, 77 (1999) 183-97.

[35] A. Manuel Stephan, Review on gel polymer electrolytes for lithium batteries, *Eur. Polym. J.*, 42 (2006) 21-42.

[36] D.T. Hallinan, N.P. Balsara, *Polymer Electrolytes*, *Annu. Rev. Mater. Res.*, 43 (2013) 503-25.

[37] Y. Alesanco, A. Vinuales, J. Rodriguez, R. Tena-Zaera, All-in-One Gel-Based Electrochromic Devices: Strengths and Recent Developments, *Materials* (Basel), 11 (2018).

[38] K. Itaya, I. Uchida, Electrochemistry of polynuclear transition metal cyanides: Prussian Blue and its analogues, *Acc. Chem. Res.*, 19 (1986) 162-8.

[39] O. Laczka, E. Baldrich, F.X. Mu oz, F.J. del Campo, Detection of Escherichia coli and Salmonella typhimurium Using Inter digitated Microelectrode Capacitive Immunosensors: The Importance of Transducer Geometry, *Anal. Chem.*, 80 (2008) 7239-47.

[40] F. Scholz, *Electroanalytical Methods. Guide to Experiments and Applications*: Springer; 2010.

[41] D. Kumar, S.A. Hashmi, Ionic liquid based sodium ion conducting gel polymer electrolytes, *Solid State Ion.*, 181 (2010) 416-23.

[42] I. Mazurenko, A. de Poulpique, E. Lojou, Recent developments in high surface area bioelectrodes for enzymatic fuel cells, *Curr. Opin. Electrochem.*, 5 (2017) 74-84.

[43] C.W. Foster, R.O. Kadara, C.E. Banks, *Screen-Printing Electrochemical Architectures*: Springer; 2016.

[44] ImageJ, <https://imagej.nih.gov/ij/>.

[45] H. Yao, A.J. Shum, M. Cowan, I. L hdesm ki, B.A. Parviz, A contact lens with embedded sensor for monitoring tear glucose level, *Biosens. Bioelectron.*, 26 (2011) 3290-6.

[46] J.R. Windmiller, J. Wang, Wearable Electrochemical Sensors and Biosensors: A Review, *Electroanalysis*, 25 (2013) 29-46.

[47] A.J. Bandonkar, W. Jia, C. Yardimci, X. Wang, J. Ramirez, J. Wang, Tattoo-Based Noninvasive Glucose Monitoring: A Proof-of-Concept Study, *Anal. Chem.*, 87 (2015) 394-8.